Observation of orientation-dependent electron transfer in molecule–surface collisions

Nils Bartels[a], Kai Golibrzuch[a], Christof Bartels[a], Li Chen[b], Daniel J. Auerbach[b], Alec M. Wodtke[a,b], and Tim Schäfer[a,1]

[a]Institut für Physikalische Chemie, Georg-August-Universität Göttingen, 37077 Göttingen, Germany; and [b]Department of Dynamics at Surfaces, Max-Planck-Institut für Biophysikalische Chemie, 37077 Göttingen, Germany

Edited* by Gerhard Ertl, Fritz-Haber-Institute, Berlin, Germany, and approved September 25, 2013 (received for review July 10, 2013)

Molecules typically must point in specific relative directions to participate efficiently in energy transfer and reactions. For example, Förster energy transfer favors specific relative directions of each molecule's transition dipole [Förster T (1948) *Ann Phys* 2(1-2):55–75] and electron transfer between gas-phase molecules often depends on the relative orientation of orbitals [Brooks PR, et al. (2007) *J Am Chem Soc* 129(50):15572–15580]. Surface chemical reactions can be many orders of magnitude faster than their gas-phase analogs, a fact that underscores the importance of surfaces for catalysis. One reason surface reactions can be so fast is the labile change of oxidation state that commonly takes place upon adsorption, a process involving electron transfer between a solid metal and an approaching molecule. By transferring electrons to or from the adsorbate, the process of bond weakening and/or cleavage is initiated, chemically activating the reactant [Yoon B, et al. (2005) *Science* 307(5708):403–407]. Here, we show that the vibrational relaxation of NO—an example of electronically nonadiabatic energy transfer that is driven by an electron transfer event [Gadzuk JW (1983) *J Chem Phys* 79(12):6341–6348]—is dramatically enhanced when the molecule approaches an Au(111) surface with the N atom oriented toward the surface. This represents a rare opportunity to investigate the steric influences on an electron transfer reaction happening at a surface.

dynamics at surfaces | orientation of molecules | rotational rainbow

The measurement of the orientation dependence of reaction rates can provide a sensitive test of theories of chemical processes. Electron transfer (ET) reactions are of particular interest in this regard, both because of the fundamental issues they pose involving subtle long-range orientation-dependent interactions, and because of the importance of ET in a remarkably wide range of phenomena. Long-range ET reactions play an important role in living systems (1). They are important in catalysis on metals and zeolites (2), in rechargeable batteries, in corrosion (3), and in photosynthesis (4).

On metal surfaces, an ET reaction may proceed by transient formation of a molecular anion via excitation of electronic states of the metal, often precluding a description of the reaction mechanism within an adiabatic picture based on the Born–Oppenheimer approximation (5, 6). As in the analogy to whaling used in naming gas-phase ET reactions, this process of an electron jump from the surface to an approaching molecule is often referred to as "harpooning" (7). There are many studies of the orientation dependence of harpooning in gas-phase reactions (8, 9), but little is known about steric influences on ET reactions during molecule–surface scattering events. An influence of N_2O orientation on exoelectron emission has been seen for reactions at alkali surfaces (10). Mechanistic studies revealed evidence for an Eley–Rideal reaction involving an ET event (11, 12). However, theoretical considerations suggest that the ET from the solid to N_2O is independent of N_2O orientation (13). To our knowledge, there is no unambiguous measurement of the orientation dependence of an ET reaction at a solid surface.

We have found a unique way to measure the orientation dependence of a simple ET reaction occurring when a molecule collides with metal surfaces. For NO colliding with a Au(111) surface, we may exploit understanding of energy transfer processes developed from years of study, both experimental and theoretical (14–18). Specifically, it is now clear that vibrational excitation and relaxation of NO colliding with a metal surface takes place via formation of a transient intermediate NO^- by ET (19). Thus, by measuring the orientation dependence of the rates of vibrational energy transfer at metal surfaces, we can probe implicitly the orientation dependence of this underlying ET reaction.

We were motivated to make these measurements by striking predictions of a recent ab initio theory that vibrational relaxation for NO(v = 15) colliding with Au(111) "N-atom first" is strongly enhanced (18). This work emphasized that dynamical steering (reorientation upon approach to the solid) could obscure orientation effects. Thus, we target measurements at high kinetic energy to have the best chance of avoiding the obscuring effects of dynamical steering. Moreover, the experiment is further simplified at high kinetic energy as these conditions suppress sticking (20), an elementary surface process where strong orientation effects have been previously reported (21–27).

The usual technique for preparing beams of oriented molecules involves state selection by focusing in an electric hexapole field (28). Unfortunately, this technique is difficult to apply at high kinetic energies. To overcome these difficulties, we used a recently developed technique, "optical state selection with adiabatic orientation," which allows us to prepare beams of oriented NO(v) molecules with kinetic energy up to and even well above 1 eV (29). It is perhaps worth noting in passing that this is an all-optical technique and, as such, does not require the long collision-free flight path used in hexapole focusing. Thus, it may be possible to extend orientation studies to higher densities

Significance

How molecules point in space—that is, their spatial orientation—determines how they interact with their environment. Exchange of energy, photons, and particles as well as chemical reactions are all elementary processes that depend on orientation. Electron transfer reactions are of particular interest because of their importance in a remarkably wide range of phenomena. In this work, we examine electron transfer reactions at surfaces, which control the change of oxidation state in surface chemistry, a critical factor explaining catalytic activity and selectivity. We report a strong orientation dependence for vibrational relaxation of a diatomic molecule colliding with a metal surface, an energy transfer process driven by electron transfer. These observations represent a challenge to modern theories of surface chemistry.

Author contributions: N.B., A.M.W., and T.S. designed research; N.B., K.G., L.C., and T.S. performed research; N.B., A.M.W., and T.S. analyzed data; and N.B., C.B., D.J.A., A.M.W., and T.S. wrote the paper.

The authors declare no conflict of interest.

*This Direct Submission article had a prearranged editor.

[1]To whom correspondence should be addressed. E-mail: tschaef4@gwdg.de.

than the high vacuum environment used here and in previous orientation experiments.

We observe a striking effect of orientation on the dynamics of vibrational energy transfer when NO($v = 3$) collides with a Au (111) surface. The survival probability of the vibrational state NO($v = 3$) after collision is a factor of 2.5 higher for molecules colliding with the O-atom first than for molecules colliding N-atom first. The rotational distribution of NO($v = 2$) resulting from vibrational relaxation is much colder than expected, reflecting a restricted approach geometry in the NO($v = 3$) collisions that result in ET and lead to vibrational relaxation. Both of these observations are direct evidence of a strong orientation effect on the underlying ET reaction controlling vibrational energy transfer.

Results

Optical State Selection with Adiabatic Orientation. In the experiment, we first generate a pulsed molecular beam with NO molecules of a kinetic energy of 0.89 eV by supersonic expansion of a mixture of 2% NO in H_2. Molecules are then vibrationally excited—$X^2\Pi_{1/2}(v' = 3, e/f) \leftarrow X^2\Pi_{1/2}(v'' = 0, e/f)Q_{11}(0.5)$—with a high-resolution infrared laser system.

The orientation is obtained by Λ-decoupling via the Stark effect in an electric field (21.4 kV/cm) between an electrode and the grounded Au surface. The orientation of the molecules can be switched rapidly by simply tuning the IR laser to excite one or the other component of the Λ-doublet. See the energy diagram in Fig. 1. A detailed explanation of this method as well as many details about the experimental setup can be found elsewhere (29).

The "uncertainty principle" prevents production of perfect orientation. Instead, we must work with an orientation probability distribution as shown in Fig. 1. The oriented NO($v = 3$) molecules then scatter from a clean Au(111) crystal at normal incidence. The collision populates many rovibrational states. After scattering, the electric field is turned off with a fast high-voltage switch. One microsecond later, rovibrational states populated by the molecule–surface collision are detected with (1+1) resonance-enhanced multiphoton ionization (REMPI) spectroscopy via the $A^2\Sigma^+(v = 0)$ state, using a UV laser.

Optical Flipping of the NO Molecule. In orientation experiments, it is often necessary and always desirable to be able to compare measured signal levels in the various (in this case, two) orientation states. With hexapoles, the orientation of a molecule may be flipped between two orientation states by changing the polarity of the orienting electric field. With the optical method presented in this paper, it is possible and furthermore quite convenient to change the orientation by tuning the IR laser used for overtone pumping between the two components of the Λ-doublet. We call this optical flipping. Corresponding REMPI spectra obtained from ionization of surface-scattered molecules when the IR laser is scanned over the Λ-doublet of the 3–0 $Q_{11}(0.5)$ transition are displayed in Fig. 2.

The dipole moment of NO vibrational states used in this work has N^-O^+ polarity. The lower frequency component of the transition (at 5,544.0039 cm^{-1}) corresponds to population of the high-field seeking state of the Λ-doublet. For a negative (positive) voltage on the orientation electrode, i.e., electric field pointing away from (toward) the Au(111) surface, this corresponds to N-first (O-first) orientation. See also Fig. 1.

In Fig. 2, both *A* and *B* show a marked dependence of the scattering signal as a function of orientation state. When the orientation field is reversed, the role of the high- and low-field–seeking states is also reversed.

IR scans like those shown in Fig. 2 not only demonstrate optical flipping, but the observed asymmetries (ratio of intensities of the two Λ-doublet transitions) also reflect directly the orientation dependence of the state-to-state scattering process. We performed many IR scans like those shown in Fig. 2 probing different rovibrational levels. The observed orientation dependence of the scattering process was entirely consistent with data obtained from UV scans (Fig. 3) at fixed IR wavelengths presented in the next section. We note that the vibrational relaxation channel NO($v = 3 \rightarrow 1$) can only be studied using the optical flipping method because the large thermal background of NO($v = 1$) molecules in the molecular beam makes an analysis of long-term UV scans unfeasible. The orientation dependence of the NO($v = 3 \rightarrow 1$) channel was found to be, within experimental error, indistinguishable from that of NO($v = 3 \rightarrow 2$) channel.

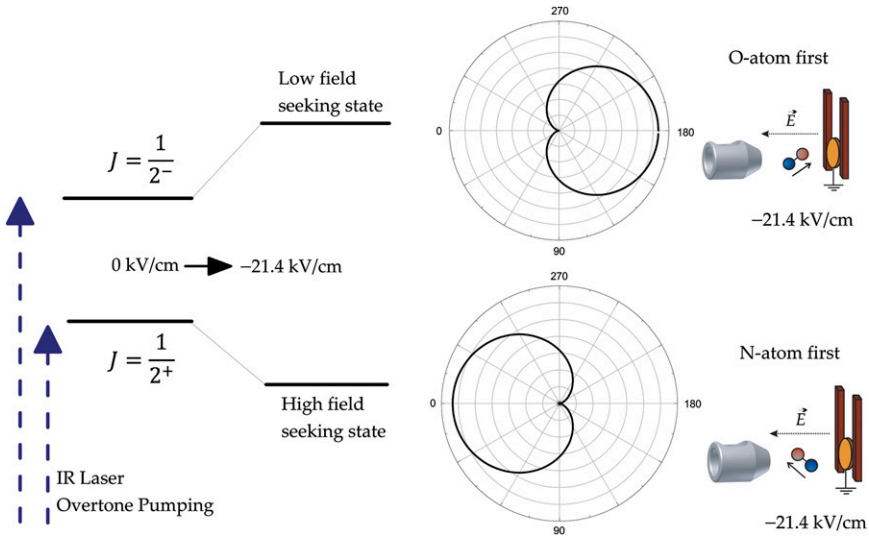

Fig. 1. Energy diagrams and orientation distributions of the NO molecule. IR overtone pumping populates one of the Λ-doublet components (– and + parity) in the $J = \Omega = 0.5$ level of $v = 3$. When the molecules enter the electric field, these components evolve adiabatically into orientated states. The polar plots show the probability distribution of these states (the applied electric field mixes the Λ-states by more than 90%) as a function of the angle θ between the NO molecule's electric dipole moment vector pointing from the negative N atom toward the positive O atom and the electric field lines (pointing from the positive surface to the negative electrode). Note that the O atom is red colored and the N atom is blue colored.

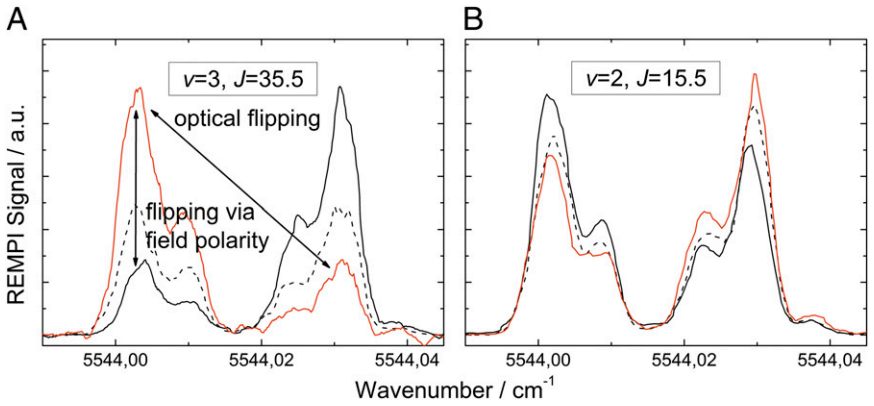

Fig. 2. Demonstration of optical flipping in NO. The figure shows the REMPI signal obtained from ionization of surface-scattered molecules when the IR laser is scanned over the Λ-doublet of the 3–0 $Q_{11}(0.5)$ transition. Measurements were performed with an orienting field of +21.4 kV/cm (positive voltage on the electrode, red solid line), −21.4 kV/cm (black solid line), and field free (black dashed line). In *A*, the REMPI laser probes the $v = 3$, $J = 35.5$ rotational level (vibrational elastic channel), and in *B*, the $v = 2$, $J = 15.5$ level (vibrational inelastic channel, detection via the $R_{11} + Q_{21}$ branch in both cases). The low-frequency component of the transition populates the high field seeker, which for a negative voltage on the orientation electrode (black line) evolves into N-down orientation. See also Fig. 1. For this component, we clearly see a suppressed survival ($v = 3 \rightarrow 3$) and an enhanced relaxation ($v = 3 \rightarrow 2$) probability. Note that the intensities of the two Λ-doublet peaks are mirrored when switching the polarity of the electrode.

Orientation Dependence of Vibrational Relaxation. Fig. 3 shows REMPI spectra obtained for the two orientations using a slightly different measurement strategy. Here, the UV laser is scanned at a fixed IR wavelength, which clearly reveals the orientation dependence of the scattering event. The lines in the spectra arise from the many rovibrational states populated in the scattering process. Because the REMPI bands used probe NO($v = 2$) and NO($v = 3$) in spectrally distinct regions, we obtain the relative vibrational state populations and its dependence on orientation by simply summing the signal over all rotational lines.

The spectra obtained for the two orientations are markedly different. The vibrational relaxation NO($v = 3 \rightarrow 2$) is clearly enhanced for "N-atom–first" collisions (Fig. 3*A*) vs. "O-atom–first" collisions (Fig. 3*B*). In addition, vibrationally elastically scattered NO($v = 3$) molecules are more strongly rotationally excited for "O-atom–first" collisions (Fig. 3*B*) and less so for "N-atom–first" collisions. In contrast NO($v = 2$) molecules exhibit almost no difference in the degree of rotational excitation for the two orientations and are also rotationally colder than NO ($v = 3$) molecules.

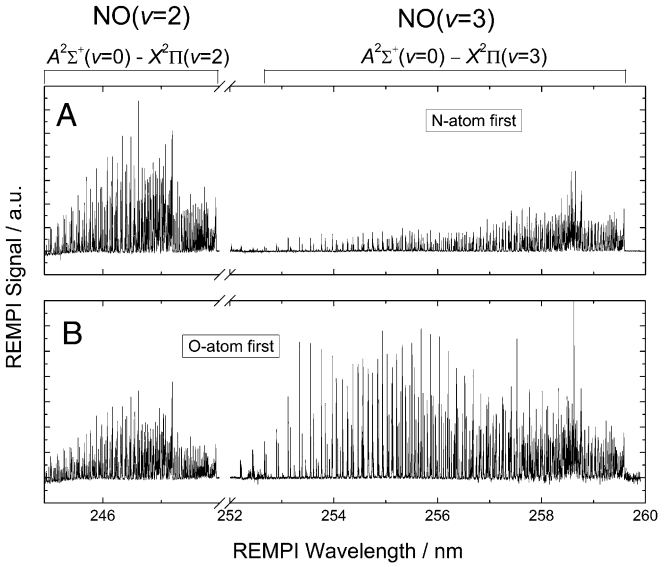

Fig. 3. (1+1)-REMPI spectra of initially oriented, surface-scattered molecules. Spectra cover the range of the $A^2\Sigma^+(v = 0) \leftarrow X^2\Pi(v = 2)$ and the $A^2\Sigma^+(v = 0) \leftarrow X^2\Pi(v = 3)$ bands (see assignment on top of spectra). (*A*) Spectrum obtained for the N-front favored orientation distribution in the incident ($v = 3$, $J = 0.5$) beam. (*B*) Spectrum obtained for the O-front favored orientation. We normalized the signal strength to the REMPI laser pulse energy.

This can be seen more directly in Fig. 4, where the state-specific population distributions derived from the spectra of Fig. 3 are shown. We extract rotational distributions from non-overlapping lines of the REMPI spectra after correcting the peak areas for Hönl–London factors, intermediate state alignment, and partial saturation effects using the expressions of Jacobs, Madix, and Zare (30). Fig. 4*A* shows the resulting population distributions averaged over different rotational branches of the $\Omega = 1/2$ state of NO($v = 3$) (vibrationally elastic) channel. Similar to previous studies, the isotropic distribution (no electric field applied, green diamonds) consists of a Boltzmann-like distribution at low values of J and a clear rotational rainbow with a distinct second maximum at a rotational energy of ∼2,600 cm^{-1} ($J \sim 40.5$) (31). This rotational rainbow is enhanced for "O-atom–first" collisions (red circles) and is weaker for "N-atom–first" collisions (blue triangles). Fig. 4*B* illustrates that the derived rotational population distributions show little change with orientation and an absence of high J excitation for the vibrationally inelastic NO($v = 2$) channel, which was already clear from examination of the spectra presented in Fig. 3.

In the *Insets* to Fig. 4, the survival probability of NO($v = 3$), P_{33}, and the NO($v = 2$) relaxation probability, P_{32}, are reported for both orientation states as well as for unoriented NO. Supplementary experiments were required to obtain these results. In a separate apparatus designed for quantitative vibrational relaxation experiments (32, 33), we measured NO vibrational state distributions for the scattering of unoriented NO($v = 3$) from Au (111) at an incidence kinetic energy of 0.96 eV, nearly identical to that used in the orientation studies. We excited NO($v = 0 \rightarrow 3$) with our Fourier transform-limited IR light source (*Materials and Methods*) and detected scattered molecules with REMPI via the $A \leftarrow X$ (0–1), (0–2), and (1–3) bands. The band spectra were integrated and corrected for differences in laser power, time-of-flight profile, scattering angular distribution and Franck–Condon factor (32, 33).

Fig. 5 presents the measured vibrational population distributions for unoriented NO (green bars). The sum of the total population appearing in different vibrational states (sum all

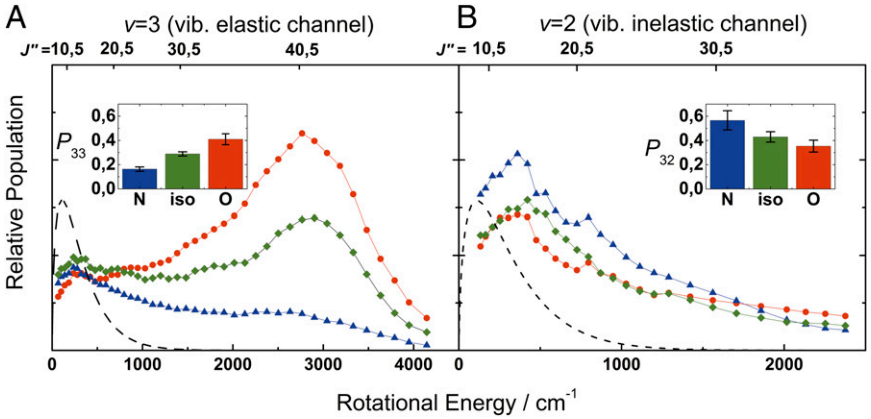

Fig. 4. Rotational and vibrational energy distributions of surface scattered molecules. (*A*) Population distributions of molecules scattered into $v = 3$, $\Omega = 0.5$ as function of the final rotational energy. Green diamonds show the isotropic distribution (no preferred orientation in the incoming molecular beam); red dots and blue triangles show the rotational distributions obtained with the O-first and N-first orientations, respectively. (*B*) Same population distributions obtained for the vibrational inelastic channel $v = 2$, $\Omega = 0.5$. The *Inset* of *A* shows the orientation-dependent NO($v = 3$) survival probability, P_{33}. The *Inset* of *B* shows the relaxation probability to $v = 2$, P_{32}. Information for these two *Insets* was obtained from experiments described in the text describing Fig. 5. The black dashed lines show rotational distributions expected for thermalized molecules at room temperature.

green bars) is constrained to unity. The vibrational state specific "O-first" to "N-first" scattering probability ratios (2.5:1 for the $v = 3 \rightarrow 3$ channel and 1:1.6 for $v = 3 \rightarrow 2$ channel) are reflected by the ratio of red-to-blue bar heights in Fig. 4. The average of these (red and blue bar) intensities is constrained to be equal to the magnitude of the unoriented (green bar) probability. The "O-first" to "N-first" scattering probability ratio for the NO($v = 3 \rightarrow 1$) relaxation channel was also found to be, within experimental error, indistinguishable from that of NO($v = 3 \rightarrow 2$), i.e., 1:1.6. For completeness and consistency, we assumed that this ratio also holds for the NO($v = 3 \rightarrow 0$) channel, although this channel does not contribute significantly to the scattering or to the analysis.

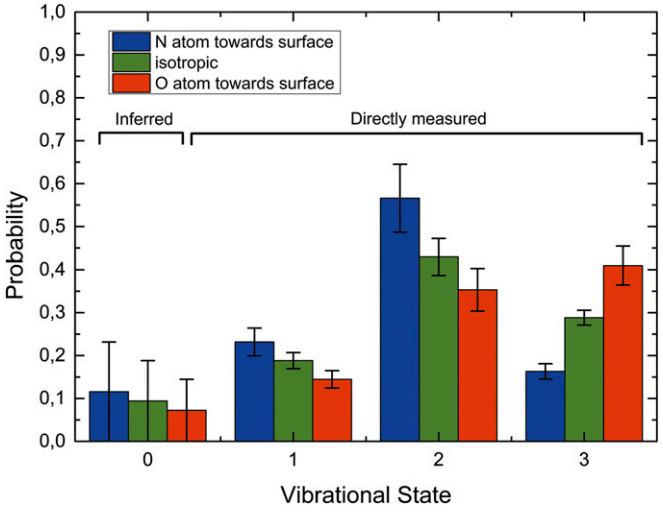

Fig. 5. Vibrational state distributions of (1) scattered unoriented NO($v = 3$) (green bars), (2) NO($v = 3$) with an incidence orientation of O atoms pointing toward the surface (red bars), and (3) NO($v = 3$) scattered with an incidence orientation of the N atoms pointing toward the surface (blue bars) from a Au(111) surface. The ratio of "O-first" scattered to "N-first" scattered molecules is 2.5:1 for vibrationally elastically scattered molecules remaining in $v = 3$ and 1:1.6 for vibrationally inelastically scattered molecules appearing in $v = 2$. A similar ratio was obtained for molecules appearing in $v = 1$. The NO($v = 0$) state population could not be measured directly due to the large NO($v = 0$) background in the molecular beam. We assumed this value to be one-half of that of NO($v = 1$), which is in accord with independent-electron surface-hopping theory that successfully reproduces the measured unoriented populations. This assumption introduces an insignificant error to the analysis.

Discussion and Conclusions

We want to bring to the reader's attention three telling features of these results:

- The total population in each vibrational state depends strongly on the initial orientation (Fig. 4, *Insets*). In particular, comparing molecules colliding with the N-atom first to those with the O-atom first, we find that the survival probability of NO($v = 3$) is reduced by a factor of 2.5 ± 0.3 for the former case in comparison with the latter and the population of NO($v = 2$ and 1) is increased by factor of 1.6 ± 0.3.
- The NO($v = 2$) spectra are rotationally colder than the corresponding NO($v = 3$) spectra. (Note that the x axes of the two panels of Fig. 4 span different energy ranges.) The pronounced rainbow structure observed in the NO($v = 3$) vibrationally inelastic channel is not present here. We exclude cooling of scattered molecules by temporary trapping on the surface as the cause of this difference because trapping is unimportant at kinetic energies above 0.1 eV (20).
- The rotational state distributions for NO($v = 2$) are almost identical for different initial orientations.

These observations can best be understood in terms of a strong angular dependence of the ET-mediated nonadiabatic gas surface interaction that drives the vibrational relaxation channel. The most direct evidence for this dependence is the strong increase in vibrationally inelastic scattering and consequent loss of NO($v = 3$) for the N-atom–first orientation. Only molecules colliding with the surface with the internuclear axis oriented in a certain angular range to the surface relax to lower vibrational states; molecules at other orientation angles are scattered with no change in vibrational state.

The differences in the degree of rotational excitation arise indirectly from this orientation dependence of vibrational relaxation. The relaxation event acts as a filter for those orientations of NO($v = 3$) with their N atoms pointed toward the surface and only these orientations efficiently relax to NO($v = 2$ and 1). Because the rotational excitation appearing in NO($v = 2$) is a function of initial orientation angle, and because NO($v = 2$)

is produced only for a certain range of initial orientations of NO($v = 3$), the rotational distribution of NO($v = 2$) is independent of the prepared orientation.

The underlying physical nature of the vibrational relaxation of NO on metal surfaces has been worked out over nearly three decades of study and is unambiguously the result of an ET event. The evidence for this is diverse and comprehensive. Interested readers are referred to a recent review (6). It includes experimental signatures in the surface temperature and incidence translational energy dependence of the probability of vibrationally state changing collisions (14, 15, 17, 34, 35). Multiquantum vibrational relaxation has been directly attributed to vibrational promotion of ET (14). Vibrationally promoted electron emission (36) exhibits a peculiar inverse velocity dependence (37), which is due to increased time available for ET at low velocity. First-principles theories that are based on an underlying ET event have captured many experimental observations for the NO Au scattering system (16, 18, 19, 38). Indeed, all modern theories of electronically nonadiabatic vibrational energy transfer for molecule surface interactions are based on ET (5), including the highly successful molecular dynamics with electron friction (39) and the independent electron surface hopping (40) approaches.

Hence, we conclude that the highlighted observations above reflect a direct measurement of the orientation dependence of a simple ET reaction involving a small molecule and a solid metal in an encounter at the surface. We further point out that the observed orientation dependence is remarkably strong. Despite the fact that the uncertainty principle blurs the initial orientation distribution, a very clear influence of orientation is seen.

We want to emphasize that our conclusions rely on an understanding of a well-studied and simple model system. Steric influences in molecule–surface interactions can be subtle, even counterintuitive. For example, the orientation dependence of the sticking of polar polyatomic molecules does not correlate with the direction of the molecular dipole moment (25–27), e.g., comparing CF_3−H and CH_3−F sticking to graphite (0001). Orientation-dependent induction forces and/or image charge interactions appear to be more important to determining the energetics of orientation in the molecule–surface collision (41, 42). Furthermore, dynamical factors must be considered, e.g., efficient T-V energy transfer for low-frequency vibrations could be orientation dependent.

Obtaining accurate information on the orientation dependence of the molecule–surface interaction potential is in principle possible using quantum chemical methods. ET and its now clearly demonstrated orientation dependence represents a challenge to these methods. It is well known that density functional theory, the most popular tool in computational surface chemistry, can lead to a poor characterization of ET (43). Weak forces like London dispersion, hydrogen bonding, induction, and/or image–charge interaction can all have a strong influence on the orientation of a molecule in its approach to a solid metal surface. Unfortunately, accurate density functional calculations of these weak forces are very expensive. In developing an accurate theoretical description of the orientation dependence of ET at solid metal interfaces, new methods will be needed. Results like those presented here provide an excellent benchmark for testing new approaches to these forefront problems in computational chemistry. We hope this work will stimulate further theoretical work to provide experimentally testable and quantitative predictions that address these matters.

Materials and Methods

The laser system used for overtone pumping provides intense Fourier transform-limited nanosecond IR pulses. A single-mode cw ring dye laser (Sirah Matisse DR; 300 mW) seeds a five-stage pulsed amplifier (Sirah Pulsed Amplifier 5×) pumped by the second harmonic of an injection seeded Nd:YAG laser (Spectra Physics Quanta Ray Pro-230-10). The Fourier transform-limited pulses (~7-ns pulse duration, 30-mJ pulse energy) are used for difference frequency mixing in a $LiNbO_3$ crystal with about 130 mJ of 1,064 nm from the injection seeded Nd:YAG laser to generate IR light at 1.8 μm (~3–4 mJ). The IR radiation is further amplified with additional 1,064 nm (~280 mJ) in an Optical Parametric Amplification process in a second $LiNbO_3$ crystal yielding up to 25 mJ per pulse of IR light with a bandwidth of less than 130 MHz. The laser beam is focused into the molecular beam with a 500-mm cylindrical lens.

The UV light used for REMPI detection is the output of a frequency-doubled visible OPO system (Continuum Sunlite Ex; 3-GHz bandwidth; 2 mJ/pulse at 250 nm). The detection takes place close to the surface and with a large beam diameter that collects molecules scattered over all possible scattering angles.

The high voltage on the orientation electrode is pulsed to ground with a high-voltage switch (Behlke; HTS 300) 1 μs before REMPI detection. Grounding the electrode allows ions produced by resonant ionization to be detected by the multichannel plate detector (Tectra MCP 050 in Chevron assembly). Furthermore, removing the orientation field ensures that REMPI detection is done in the absence of a Stark effect that might introduce complications in the data analysis.

Before scattering measurements are carried out, the Au(111) crystal is cleaned by sputtering with an Ar-ion gun (LK Technologies; NGI3000). The surface is then annealed for 20 min at 870 K, and surface cleanliness is verified with Auger electron spectroscopy.

ACKNOWLEDGMENTS. We thank Alexander Kandratsenka for useful discussions. A.M.W. and D.J.A. acknowledge The Alexander von Humboldt Foundation for support.

1. Balabin IA, Onuchic JN (2000) Dynamically controlled protein tunneling paths in photosynthetic reaction centers. *Science* 290(5489):114–117.
2. Yoon KB (1993) Electron-transfer and charge-transfer reactions within zeolites. *Chem Rev* 93(1):321–339.
3. Balzani V (2008) Front matter. *Electron Transfer in Chemistry*, ed Balzani V (Wiley-VCH, Weinheim, Germany), pp i–lxxx.
4. Barbara PF, Meyer TJ, Ratner MA (1996) Contemporary issues in electron transfer research. *J Phys Chem* 100(31):13148–13168.
5. Gadzuk JW (1983) Vibrational excitation in molecule–surface collisions due to temporary negative molecular ion formation. *J Chem Phys* 79(12):6341–6348.
6. Wodtke AM, Matsiev D, Auerbach DJ (2008) Energy transfer and chemical dynamics at solid surfaces: The special role of charge transfer. *Prog Surf Sci* 83(3):167–214.
7. Kleyn AW (1990) Harpooning and chemistry at surfaces. *AIP Conference Proceedings* (American Institute of Physics, Melville, NY), No. 205, pp 451–457.
8. Brooks PR (2012) Electron transfer, harpooning, reagent orientation, and chemical intuition. *Mol Phys* 110(15–16):1729–1738.
9. Wiskerke AE, Stolte S, Loesch HJ, Levine RD (2000) $K+CH_3I \rightarrow KI+CH_3$ revisited: The total reaction cross section and its energy and orientation dependence. A case study of an intermolecular electron transfer. *Phys Chem Chem Phys* 2(4):757–767.
10. Brandt M, Greber T, Böwering N, Heinzmann U (1998) The role of molecular state and orientation in harpooning reactions: N_2O on Cs/Pt(111). *Phys Rev Lett* 81(11):2376–2379.
11. Brandt M, Greber T, Kuhlmann F, Böwering N, Heinzmann U (1998) State- and orientation-dependent N_2 emission in the N_2O+Cs reaction. *Surf Sci* 402-404(0):160–164.
12. Brandt M, Kuhlmann F, Greber T, Böwering N, Heinzmann U (1999) Interaction of gas-phase oriented N_2O with lithium metal: Evidence for an Eley–Rideal mechanism. *Surf Sci* 439(1-3):49–58.
13. Suter HU, Greber T (2004) On the dissociation of N_2O after electron attachment. *J Phys Chem B* 108(38):14511–14517.
14. Huang Y, Rettner CT, Auerbach DJ, Wodtke AM (2000) Vibrational promotion of electron transfer. *Science* 290(5489):111–114.
15. Huang Y, Wodtke AM, Hou H, Rettner CT, Auerbach DJ (2000) Observation of vibrational excitation and deexcitation for NO ($v = 2$) scattering from Au(111): Evidence for electron-hole-pair mediated energy transfer. *Phys Rev Lett* 84(13):2985–2988.
16. Newns DM (1986) Electron-hole pair mechanism for excitation of intramolecular vibrations in molecule surface scattering. *Surf Sci* 171(3):600–614.
17. Rettner CT, Fabre F, Kimman J, Auerbach DJ (1985) Observation of direct vibrational excitation in gas-surface collisions: NO on Ag(111). *Phys Rev Lett* 55(18):1904–1907.
18. Shenvi N, Roy S, Tully JC (2009) Dynamical steering and electronic excitation in NO scattering from a gold surface. *Science* 326(5954):829–832.
19. Cooper R, et al. (2012) Multiquantum vibrational excitation of NO scattered from Au(111): Quantitative comparison of benchmark data to ab initio theories of nonadiabatic molecule-surface interactions. *Angew Chem Int Ed* 51(20):4954–4958.
20. Wodtke AM, Yuhui H, Auerbach DJ (2005) Insensitivity of trapping at surfaces to molecular vibration. *Chem Phys Lett* 413(4-6):326–330.
21. Fecher GH, Böwering N, Volkmer M, Pawlitzky B, Heinzmann U (1990) Dependence of the sticking probability on initial molecular orientation: NO on Ni(100). *Surf Sci* 230(1-3):L169–L172.

22. Müller H, et al. (1992) Collision of oriented NO with Ni(100) and with oriented CO on Ni(100). *Surf Sci* 269–270:207–212.
23. Fecher GH, Volkmer M, Pawlitzky B, Böwering N, Heinzmann U (1990) Orientation dependence of the sticking probability of NO at Ni(100). *Vacuum* 41(1-3):265–268.
24. Müller H, Zagatta G, Böwering N, Heinzmann U (1994) Orientation dependence of NO sticking and scattering at Pt(100). *Chem Phys Lett* 223(3):197–201.
25. Mackay RS, Curtiss TJ, Bernstein RB (1989) Determination of preferred orientation for sticking of polar-molecules in beams incident on a graphite (0001) surface. *Chem Phys Lett* 164(4):341–344.
26. Curtiss TJ, Bernstein RB (1989) Steric effect in the scattering of oriented CH_3F molecules by graphite (0001). *Chem Phys Lett* 161(3):212–218.
27. Mackay RS, Curtiss TJ, Bernstein RB (1990) Strong orientation dependence of the scattering of fluoroform by graphite (0001). *J Chem Phys* 92(1):801–802.
28. Kramer KH, Bernstein RB (1965) Focusing and orientation of symmetric-top molecules with electric six-pole field. *J Chem Phys* 42(2):767–770.
29. Schäfer T, Bartels N, Hocke N, Yang X, Wodtke AM (2012) Orienting polar molecules without hexapoles: Optical state selection with adiabatic orientation. *Chem Phys Lett* 535:1–11.
30. Jacobs DC, Zare RN (1986) Reduction of 1+1 resonance enhanced MPI spectra to populations and alignment factors. *J Chem Phys* 85(10):5457–5468.
31. Geuzebroek FH, et al. (1991) Rotational-excitation of oriented molecules as a probe of molecule surface interaction. *J Phys Chem* 95(21):8409–8421.
32. Bartels C, et al. (2012) Vibrational excitation and relaxation of NO molecules scattered from a Au(111) surface. *28th International Symposium on Rarefied Gas Dynamics 2012*, Vols 1 and 2, *AIP Conference Proceedings*, eds Mareschal M, Santos A (American Institute of Physics, Melville, NY), Vol 1501, pp 1330–1339.
33. Cooper R, et al. (2012) On the determination of absolute vibrational excitation probabilities in molecule-surface scattering: Case study of NO on Au(111). *J Chem Phys* 137(6):064705.
34. Watts EK, Siders JLW, Sitz GO (1997) Vibrational excitation of NO scattered from Cu (110). *Surf Sci* 374(1-3):191–196.
35. Bartels C, Cooper R, Auerbach DJ, Wodtke AM (2011) Energy transfer at metal surfaces: The need to go beyond the electronic friction picture. *Chem Sci* 2(9): 1647–1655.
36. White JD, Chen J, Matsiev D, Auerbach DJ, Wodtke AM (2005) Conversion of large-amplitude vibration to electron excitation at a metal surface. *Nature* 433(7025): 503–505.
37. Nahler NH, White JD, Larue J, Auerbach DJ, Wodtke AM (2008) Inverse velocity dependence of vibrationally promoted electron emission from a metal surface. *Science* 321(5893):1191–1194.
38. Monturet S, Saalfrank P (2010) Role of electronic friction during the scattering of vibrationally excited nitric oxide molecules from Au(111). *Phys Rev B Condens Matter* 82(7):075404-1–075404-10.
39. Head-Gordon M, Tully JC (1995) Molecular-dynamics with electronic frictions. *J Chem Phys* 103(23):10137–10145.
40. Shenvi N, Roy S, Tully JC (2009) Nonadiabatic dynamics at metal surfaces: Independent-electron surface hopping. *J Chem Phys* 130(17):174107.
41. Whitehouse DB, Buckingham AD, Bernstein RB, Cho VA, Levine RD (1991) Orientation dependence of the induction contribution in molecule graphite interactions. *J Phys Chem* 95(21):8175–8177.
42. Ionova IV, Ionov SI, Bernstein RB (1991) An image charge model for the classical trajectory simulations of molecule surface scattering—steric effects in the scattering of CHF_3 on graphite(0001). *J Phys Chem* 95(21):8371–8376.
43. Libisch F, Huang C, Liao P, Pavone M, Carter EA (2012) Origin of the energy barrier to chemical reactions of O_2 on Al(111): Evidence for charge transfer, not spin selection. *Phys Rev Lett* 109(19):198303.